

# TEMPORAL AND SPATIAL VARIATIONS OF THE ATMOSPHERIC DIFFUSE LIGHT

S. M. KWON<sup>1</sup>, S. S. HONG<sup>1</sup>, AND J. L. WEINBERG<sup>2</sup>

<sup>1</sup>*Department of Astronomy, Seoul National University, 151-742, KOREA*

<sup>2</sup>*Space Astronomy Laboratory, University of Florida, U.S.A.*

**ABSTRACT.** The Barbier's relation for the diffusely scattered airglow has been modified in such a way that it may describe, with simple changes of two parameter values, the dependence on zenith distance of the atmospheric diffuse light at any time of the night.

## 1. Introduction

The atmosphere related diffuse light (ADL) is composed of the directly transmitted airglow (AG) and the diffusely scattered signals of integrated starlight (IS), zodiacal light (ZL) and the AG. Conditions in the AG emitting layer are known to vary with time during a night (Tanabe 1964; Dumont 1965; cf. Roach and Gordon 1972; Tanaka *et al.* 1989). Changing configurations of the Milky Way and the ZL-cone with respect to the earth scattering atmosphere further make the ADL vary with time and sky position.

For the reduction of ZL, many methods have been devised to remove the ADL from the observed sky brightness (Weinberg 1963; Dumont 1965; Dumont and Sanchez 1975; Hong *et al.* 1985). To avoid the errors due to the time-variation, observed data were often averaged over the period extending many years. The averaging was successful in rendering overall pictures of the zodiacal dust cloud; it also masked valuable information about the detailed structures of the cloud.

## 2. Reduction of the ADL from the Night Sky Observations

Weinberg and Mann monitored the night sky brightness at 5080Å and 5300Å, by scanning the meridian eleven times over a night for each of the wavelengths. To characterize the dependencies of the ADL brightness on time  $t$  and zenith distance  $z$ , we analyzed this set of 22 meridian scans in the same way as done for the almucantar scans (Kwon, Hong, Weinberg and Misconi 1991, in this volume).

An example of the scans after being calibrated is shown in Fig 1 by dots; the ordinate represents the brightness in units of  $S_{10}(V)_{G2V}$ , and the abscissa the zenith distance in degrees. By summing up the directly transmitted contributions from resolved bright stars, IS (Toller 1981), and ZL (Levasseur-Regourd and Dumont 1980), we synthesized the profile of directly transmitted astronomical light only.

The difference between the observed (dots) and the synthetic (thin line) profiles gives the brightness of the ADL along the meridian, and is shown by the thick solid line in the figure. We drew a smooth line through the sharp spikes due to imperfect removals of the bright stars. Reading

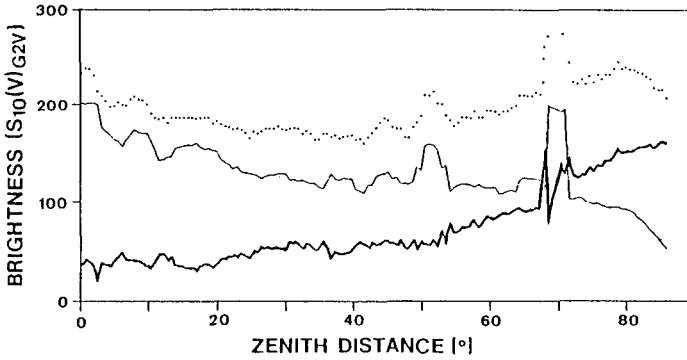


Fig 1 - A sample plot of the meridian scan simulations. Solid dots represent the observed brightness distribution and the thin solid curve represents the synthetic profile. The difference between the two curves is plotted in a thick line, which represents the ADL brightness.

the brightness off the smoothed line, we have constructed a two-dimensional ( $t, z$ ) ADL table for each of the wavelengths. Figures 2a (5080Å) and 2b(5300Å) illustrate how the ADL varies with  $t$  at a few selected zenith distances.

The ADL brightness increases rather rapidly in the beginning of the night, reaches a broad maximum extending 21 to 22 hr in Hawaii standard time (HST), and declines slowly afterwards. This trend of variation is the same for the both wavelengths. The amplitude of the time-variation generally increases with increasing  $z$ , and becomes as large as  $30 S_{10}(V)_{G2V}$  at  $z \simeq 80^\circ$ . This big an amplitude makes time-dependent corrections be necessary for the ADL.

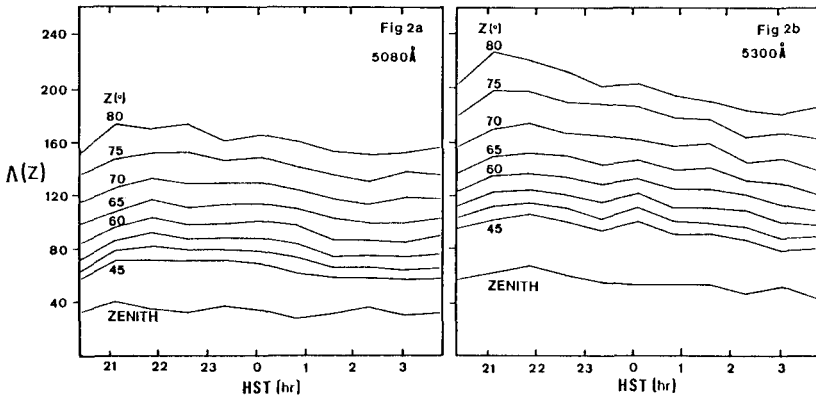


Fig 2 - Time variations of the ADL are shown for wavelength 5080Å(a), and 5300Å(b).

At a given time, brightness  $\Lambda(z)$  of the ADL increases with  $z$  up to  $80^\circ$ , where it reaches a maximum and reverses its rising trend. We normalized the brightness profile to its zenith brightness  $\Lambda_0$ , which is about 40 and 50  $S_{10}(V)_{G2V}$  at 5080Å and 5300Å, respectively. A sample of the normalized profiles is shown in Fig 3 by dots. General pattern of the variation seen in the figure persists for all the 22 profiles; only maximum values are different depending on the time of observation. It would

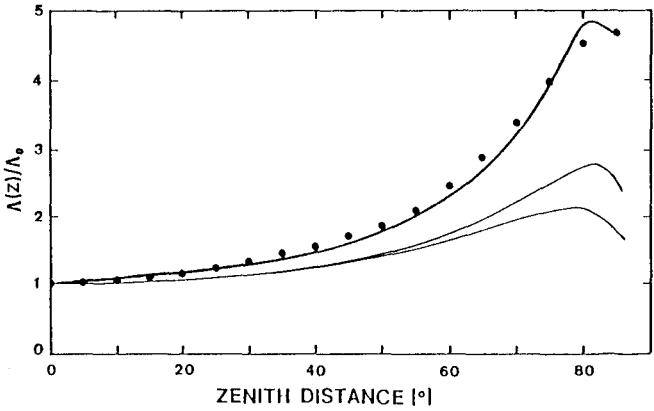


Fig 3 - Normalized distribution of the ADL brightness with zenith distance. The observed ADL is shown by the filled circles, and the non-linear least squares fit of the modified Barbier's relation to the data is represented by the thick solid line. The two thin curves are calculated from the original version of the Barbier's relation with  $h = 50$  and  $200$  km.

then be convenient, if one could describe the normalized profiles by a simple function of  $z$  with a few parameters.

**3. Parametric Representation of the Normalized ADL Profile**

Barbier (1944) attempted to describe the  $z$ -dependence of the diffusely scattered AG with the function  $(F_1 - F_2 \cos^2 z) \{ 1 - \exp[-\tau_1 x] \}$ , where  $F_1$  and  $F_2$  are parameters related to the height  $h$  of the AG emitting layer,  $\tau_1$  is the scattering optical depth at the zenith, and  $x$  is the airmass at  $z$ . When Dumont (1965) formulated his multiple height method (cf. Dumont and Sanchez 1975), he used the Barbier's relation to conceptualize the  $z$ -dependence of the diffusely scattered AG. We use this relation not because of its accuracy but because of its flexibility. The components in the ADL other than the diffusely scattered AG require the original Barbier's relation to be modified.

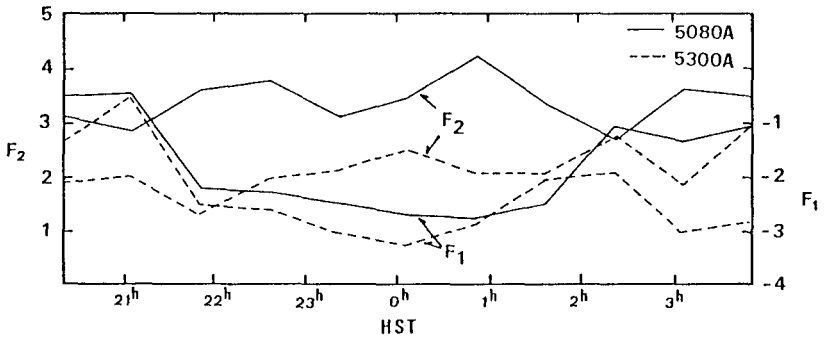


Fig 4 - The time dependent variations of the parameter  $F_1$  and  $F_2$  are plotted as functions of HST for the two wavelengths.

If  $\theta$  denotes the angle between a line of sight and the outward normal drawn at the point where the line of sight enters the AG emitting layer, the pathlength through the layer becomes proportional to  $\sec \theta$ . The intensity of the AG incident upon the earth absorbing and scattering atmosphere is assumed proportional to the pathlength;  $\sec \theta$  is another representation of the van Rhijn function. The directly transmitted AG may then be modeled by  $\sec \theta \exp[-\tau_0 x]$  with  $\tau_0$  being the extinction optical depth of the atmosphere at the zenith. For  $h = \infty$ ,  $F_1 = 0.5$  and  $F_2 = 0$ . Consequently, the diffusely scattered components of the IS and ZL are easily incorporated

into the Barbier's relation by simply relaxing the definition of  $F_1$ . We thus propose  $\Lambda(z)/\Lambda_0 = \sec \theta \exp[-\tau_0 x] + (F_1 - F_2 \cos^2 z) \{1 - \exp[-\tau_1 x]\}$  as an empirical function to describe the meridian profile of the normalized ADL at a fixed time.

In the analysis of night sky observations, Dumont (1965) is the first who differentiated the scattering  $\tau_1$  from the extinction  $\tau_0$  optical depth. For the night Kwon (1990) was able to determine  $\tau_0$  and  $\tau_1$  as functions of time. Therefore, the two optical depths are not free parameters.

Since  $\theta$  is related to  $z$  through a known function of  $h$  and Barbier gave  $F_1$  and  $F_2$  as functions of  $h$  only, in a strict sense of Barbier, the trial relation we propose could be a single parameter function. The two curves in the lower part of Fig 3 illustrate the range one can have by changing  $h$  from 50 to 200 km in the original definitions of  $F_1$  and  $F_2$ . Comparison of the curves with the observed profile clearly suggests that the meanings Barbier originally envisioned may no longer be attributed to  $F_1$  and  $F_2$ ; we thus decided to treat  $F_1$  and  $F_2$  as free parameters and to simply approximate  $\theta$  to  $z$ , limiting the number of free parameters to only two.

With the method of non-linear least squares fit, we determined the best  $F_1$  and  $F_2$  values for each profile. An example of such fits is shown in Fig 3 by the thick solid line. The best parameter values are shown in Fig 4 as functions of time for the both wavelengths.

The best fit values of  $F_1$  and  $F_2$  turned out to be outside the ranges that are allowable from Barbier's original definitions of them. We consider our trial function as a mathematical means for simply reproducing the  $z$ -dependence of the observed ADL. The modified Barbier's relation accurately reproduces the  $z$ -dependence of the observed profile, and is flexible enough to give equally good fits for all the 22 profiles.

#### 4. Conclusion

The brightness of ADL varies over a night to the degree that its corrections are to be made time-dependently. The Barbier's relation has been modified to describe the  $z$ -dependence of the ADL at a fixed time. We propose the modified Barbier's relation with time-dependent values of  $F_1$  and  $F_2$  as a practical means for effecting the time-dependent ADL corrections.

SSH and SMK were supported by the Basic Science Research Institute Program, Korean Ministry of Education. At an earlier stage, JLW and SMK were partially supported by the US AFOSR.

#### REFERENCES

- Barbier, D. 1944, *Ann. Geophys.*, **1**, 144  
 Dumont, R. 1965, *Ann. d'Astrophys.*, **28**, 265  
 Dumont, R., and Sanchez, F. 1975, *Astr. Ap.*, **38**, 397  
 Hong, S. S., Misconi, N. Y., van Dijk, M. H. H., Weinberg, J. L. and Toller, G. N. 1985, in *Properties and Interactions of Interplanetary Dust*, ed. R. H. Giese and P. Lamy (Dordrecht:Reidel), p.33  
 Kwon, S. M. 1990, *Ph. D. Thesis*, Seoul National University  
 Levasseur-Regourd, A. C. and Dumont, R. 1980, *Astr. Ap.*, **84**, 227  
 Roach, F. E. and Gordon, J. L. 1972, *The Light of the Night Sky*, (Dordrecht:Reidel)  
 Tanabe, H. 1964, *Publ. Astron. Soc. Japan*, **16**, 324  
 Tanaka, K., Miyashita, A., Takechi, A. and Tanabe, H. 1989, *Atlas of Zenith 5300Å Brightness*, National Astronomical Observatory, Japan  
 Toller, G. N. 1981, *Ph. D. Thesis*, State University of New York at Stony Brook  
 Weinberg, J. L. 1963, *Ph. D. Thesis*, University of Colorado